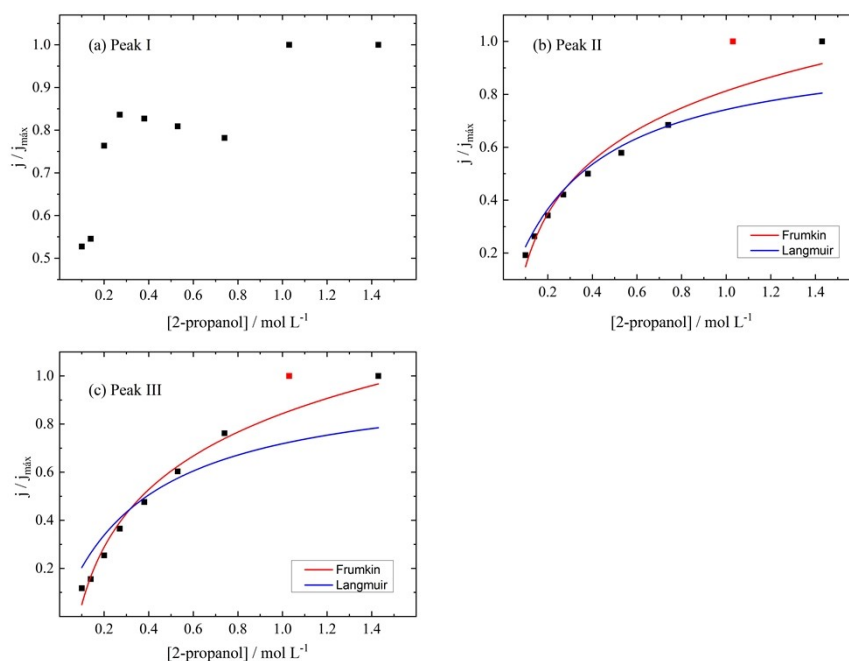


- Supplementary Information for -

## The oscillatory electro-oxidation of 2-propanol on platinum: the effect of temperature and of the addition of methanol

Gianluca Ragassi, André H. B. Dourado, Hamilton Varela

São Carlos Institute of Chemistry, University of São Paulo, PO Box 780, 13560-970, São Carlos, SP, Brazil



**Figure S1.** Adsorption isotherms obtained for the 2-propanol on Pt considering the peak current as proportional to the coverage degree. The blue lines consist of the Lagmuir equation adjustment and the red of the Frumkin one. Support electrolyte: aqueous solution containing  $[\text{H}_2\text{SO}_4] = 0.1 \text{ mol L}^{-1}$ .

The Langmuir adsorption isotherm is presented as Equation S1.

$$\theta / ((1 - \theta)) = KC \quad \text{Equation S1}$$

Where  $\theta$  is the coverage degree, K the adsorption equilibrium constant and C the 2-propanol concentration. After isolating  $\theta$ , one obtains Equation S2.

$$\theta = KC / (1 + KC) \quad \text{Equation S2}$$

In the Langmuir adsorption isotherm is one of the most applied adsorption models, and the simplest one. It considers a constant adsorption energy during the electrode coverage process, which means that the adsorbed species does not interfere in the continuity of the process, and that all adsorption sites are equivalent.

Frumkin,<sup>1</sup> proposed a different adsorption model. Observing that the adsorption energy would be affected by the adsorption site and/or by the already adsorbed species. The overall law is presented in Equation S3.

$$\theta/(1 - \theta)\exp(r\theta/RT) = K_0C \quad \text{Equation S3}$$

The new variables considered by Frumkin are  $K_0$ , the equilibrium constant observed at null coverage and  $r$ , which is known as the heterogeneity factor. This last one quantifies the change in the adsorption energy with the coverage, assuming that this dependence is linear, as shown in Equation S4.

$$\Delta G_\theta = \Delta G_0 + r\theta \quad \text{Equation S4}$$

Where  $\Delta G_\theta$  is the adsorption energy at the coverage degree  $\theta$  and  $\Delta G_0$  is the adsorption energy at the free surface. Naturally, it can be observed that if the adsorbed species has low interaction,  $r$  is close to zero, so the Langmuir model (Equations S1-S2) can be obtained.

When the coverage degree is at the limits of  $\theta$  going to zero, or one, the homogeneity of the surface can be observed, so the adsorption energy changes at low dependence on  $\theta$ , so at these physical limits, the Langmuir model can be used. In this way, the Frumkin model can be better applied when  $\theta/(1 - \theta)$  is close to the unity, so Equation S3 is normally resumed in Equation S5

$$\theta = RT/r \ln(K_0C) \quad \text{Equation S5}$$

Equation S5 was the one used for the adjustments presented in Figure S1. By these fittings, it can be observed just one value of  $r$ , 8.6 kJ mol<sup>-1</sup>. The positive  $r$  suggests a repulsive interaction between the adsorbed species. With this and according with Equation S4, the adsorption energy will be less negative with increment of  $\theta$ , and the adsorbed species will probably not cover the whole surface. The obtained  $r$  is very low, if compared with the typical adsorption from gas phase, which is around 150 kJ mol<sup>-1</sup>, or the expected electrochemical values, which for strong interactions normally present  $r$  around 60 kJ mol<sup>-1</sup>.<sup>2</sup> Even with the low interaction the adsorption energy changes with  $\theta$  is significant for the 2-propanol, so the Langmuir model is not well adjusted to the system. In addition, the same value being observed independent on the oxidative peak used suggests that the same adsorbed intermediate is generated/consumed at the rate limiting step at those processes.

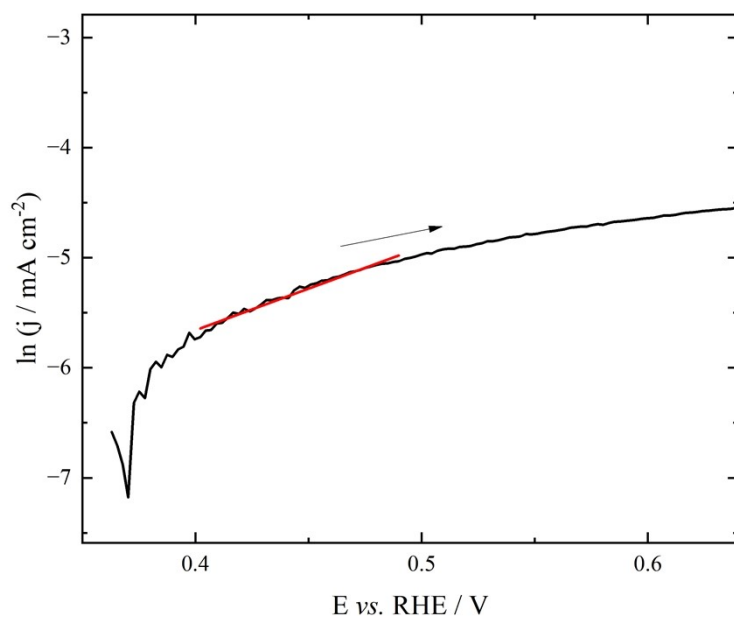


**Figure S2:** Tafel plot for electro-oxidation of 2-propanol on Pt at  $0.002 \text{ V s}^{-1}$ . The value obtained for  $n(1-\alpha)$  was 0,45. Electrolyte: aqueous solution containing  $[\text{H}_2\text{SO}_4] = 0.1 \text{ mol L}^{-1}$  and  $[\text{H}_3\text{C-HCOH-CH}_3] = 1.0 \text{ mol L}^{-1}$ .

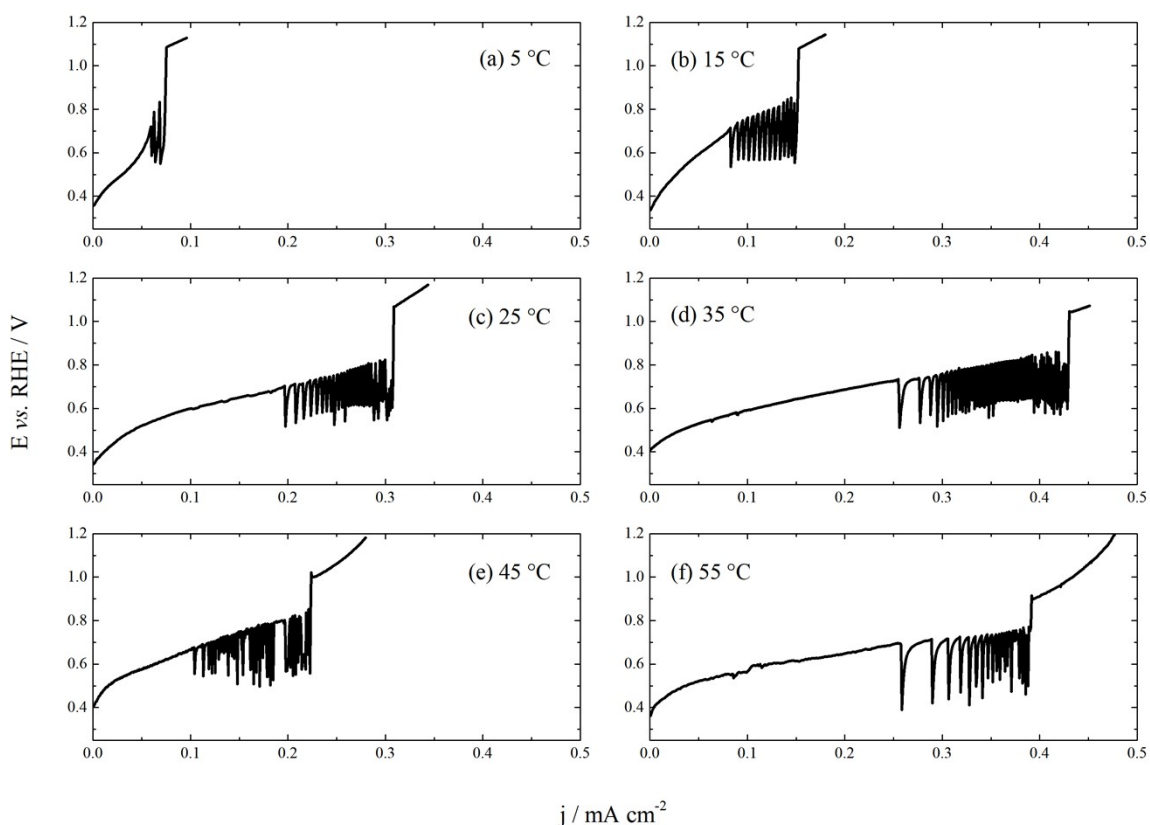


**Figure S3:** Galvanodynamic sweeps ( $dl/dt = 15 \text{ nA s}^{-1}$ ) at (a)  $5 \text{ }^\circ\text{C}$ , (b)  $15 \text{ }^\circ\text{C}$ , (c)  $25 \text{ }^\circ\text{C}$ , (d)  $35 \text{ }^\circ\text{C}$ , (e)  $45 \text{ }^\circ\text{C}$  and (f)  $55 \text{ }^\circ\text{C}$ . Electrolyte: aqueous solution containing  $[\text{H}_2\text{SO}_4] = 0.1 \text{ mol L}^{-1}$  and  $[\text{H}_3\text{C-HCOH-CH}_3] = 1.0 \text{ mol L}^{-1}$ .

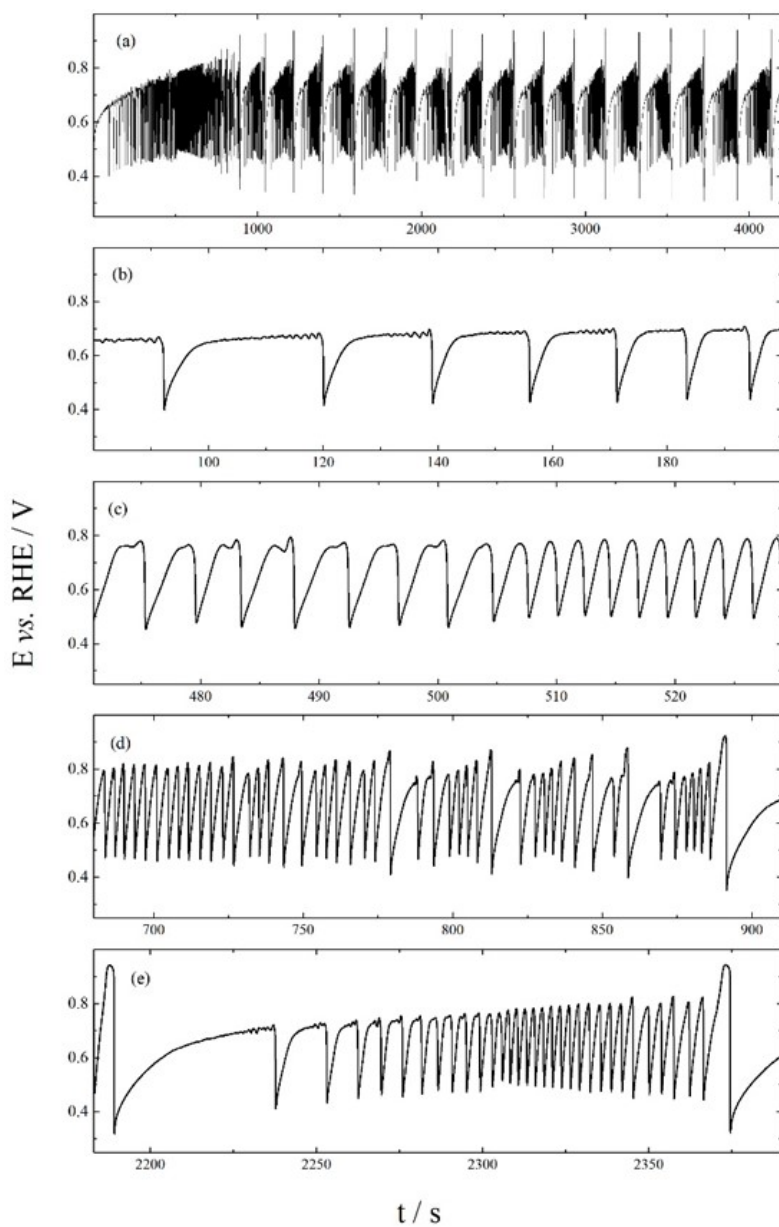


**Figure S4:** time-evolution of the potential oscillations recorded at  $j = 0.40 \text{ mA.cm}^{-2}$  and at  $60 \text{ }^\circ\text{C}$ . Electrolyte: aqueous solution containing  $[\text{H}_2\text{SO}_4] = 0.1 \text{ mol L}^{-1}$  and  $[\text{H}_3\text{C-HCOH-CH}_3] = 1.0 \text{ mol.L}^{-1}$ . The number of small amplitude and high frequency oscillations intercalated by large amplitude ones displayed in (a) are 30, 32, 30, 34, 33, 30, 36, 32, 32, 26, 28, 32, 33, 30, 30, 30, 36.

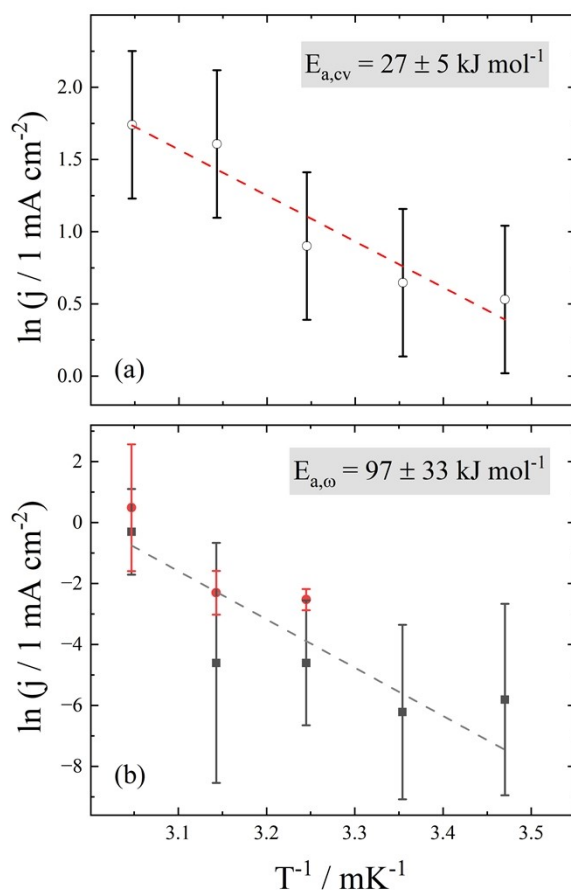


**Figure S5:** Arrhenius plots using the (a) voltametric peak current density, and (b) oscillatory frequency, where black and red is associated to type 1 and type 2 oscillations, respectively. The oscillatory frequency considered for this plot was the average value measured for the three initial oscillatory cycles at of each type group. Electrolyte: aqueous solution containing  $[\text{H}_2\text{SO}_4] = 0.1 \text{ mol L}^{-1}$  and  $[\text{H}_3\text{C-HCOH-CH}_3] = 1.0 \text{ mol L}^{-1}$ .

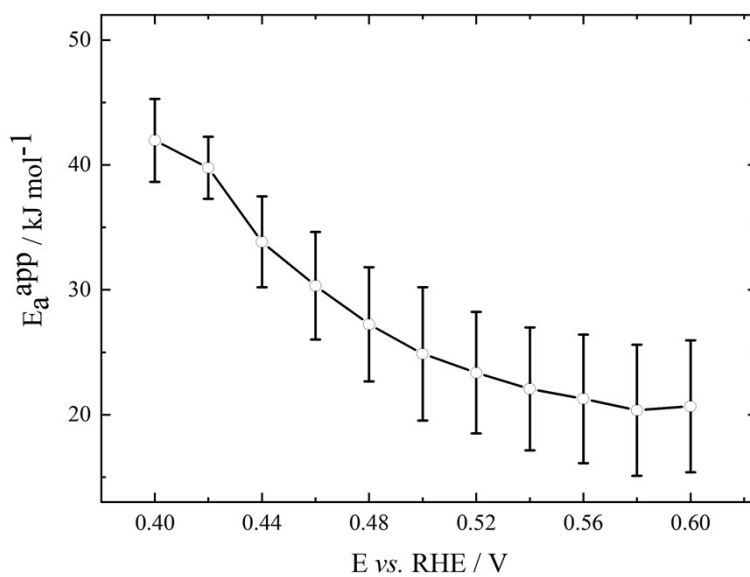


**Figure S6:** Apparent activation energy ( $E_a^{\text{app}}$ ) vs. potential applied ( $E$ ) vs. RHE. Electrolyte: aqueous solution containing  $[\text{H}_2\text{SO}_4] = 0.1 \text{ mol L}^{-1}$  and  $[\text{H}_3\text{C-HCOH-CH}_3] = 1.0 \text{ mol L}^{-1}$ .

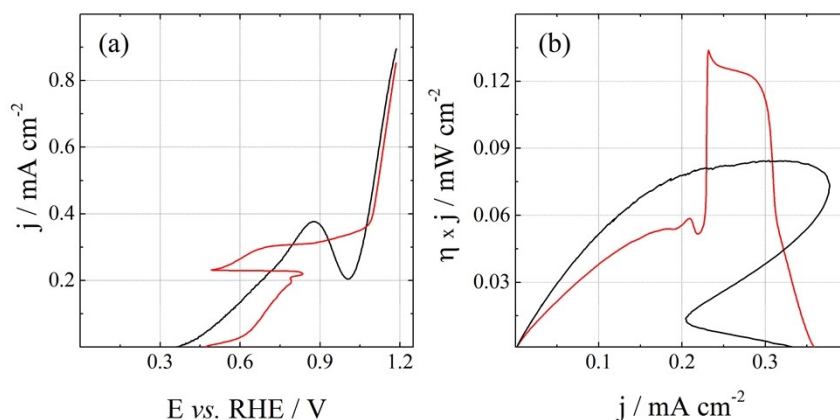


**Figure S7:** (a) Linear potential sweep (black line,  $dE/dt = 2 \text{ mV s}^{-1}$ ) and current sweep (red line,  $dI/dt = 5 \text{ } \mu\text{A s}^{-1}$ ) for the electro-oxidation of 2-propanol and (b) the corresponding power density vs. current density curves under potentiostatic (black) and galvanodynamic (red) regimes at  $25 \text{ }^\circ\text{C}$ . Electrolyte: aqueous solution containing  $[\text{H}_2\text{SO}_4] = 0.1 \text{ mol L}^{-1}$  and  $[\text{H}_3\text{C-HCOH-CH}_3] = 1.0 \text{ mol L}^{-1}$ .

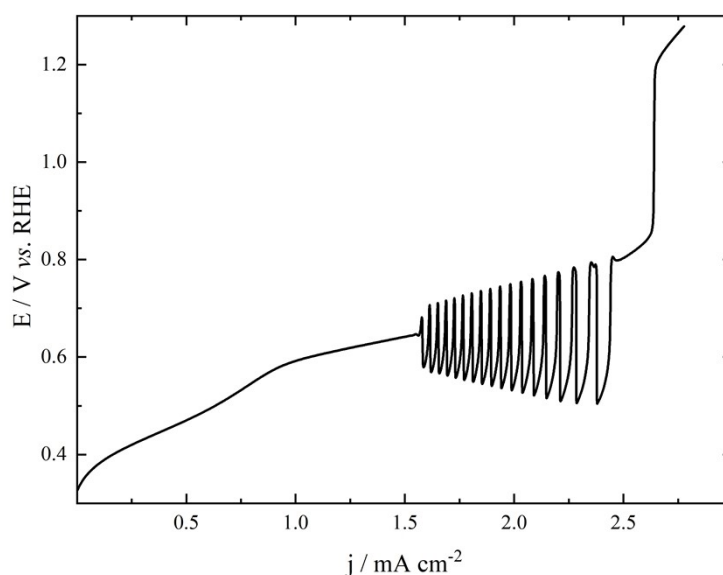


**Figure S8:** Galvanodynamic sweeps ( $dI/dt = 5 \text{ } \mu\text{A s}^{-1}$ ) at  $25 \text{ }^\circ\text{C}$ . Electrolyte: aqueous solution containing  $[\text{H}_2\text{SO}_4] = 0.1 \text{ mol L}^{-1}$ ,  $[\text{H}_3\text{C-HCOH-CH}_3] = 1.0 \text{ mol L}^{-1}$  and  $[\text{H}_3\text{COH}] = 0.5 \text{ mol L}^{-1}$ .

Knowing that all peaks lead to a Frumkin isotherm (Figure S1), and that the Tafel slope (Figure S2) indicated a reversible and mono-electronic rate determinant step, we decided to further investigate the process by applying several scan rates during the voltammetric cycles. In this way, we can obtain information regarding the mass transport, if the peak currents are linearized by the square root of the scan rate. As presented in Figure S9).

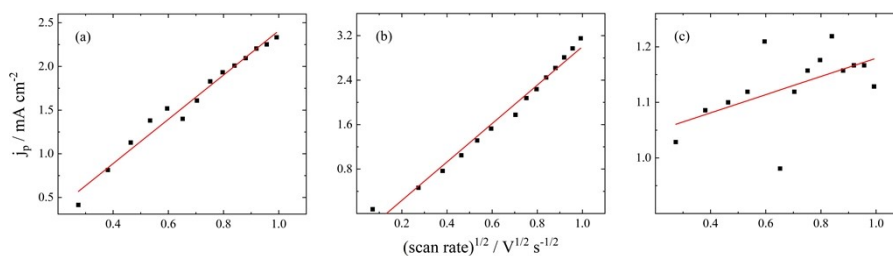


**Figure S9:**  $j_p$  vs. square root of scan rate plot for peaks (a) I, (b) II and (c) III. Electrolyte: aqueous solution containing  $[\text{H}_2\text{SO}_4] = 0.5 \text{ mol L}^{-1}$  and  $[\text{H}_3\text{C-HCOH-CH}_3] = 1.0 \text{ mol L}^{-1}$ .

Despite having good statistical information about the  $R^2$ , for none of these peaks the Randles-Sevcik equation provided a satisfactory adjustment. From the first peak, one can suggest that two linear regions, one at lower and another at higher scan rates, with some outliers at intermediate rates is obtained, however, this would indicate a change in the number of electrons transferred or in the diffusion coefficient, these assumptions do not make sense, since the mechanism proposed in the literature would suggest just 2-propanol and acetone as reactants and products, in order. For the second peak, some curvature in the points can be observed, in a way that the points start “higher” than the linear fit, became lower and then, once again higher. For the third peak the poor linear fit is evident for the random point distribution around the fit. Another possible linear adjustment that can be done is based on the model proposed by Srinivasan and Gileadi,<sup>3</sup> in which the adsorption pseudocapacitance is considered. In this way, the peak currents are adjusted as a linear dependence on the scan rate (Figure S10) and if this is true, the mass transport limitation is not the main reason for such charge transfer control, the kinetics limitations are also present and, in this case, the peak potential would be a linear function of  $\log v$  (Figure S11).

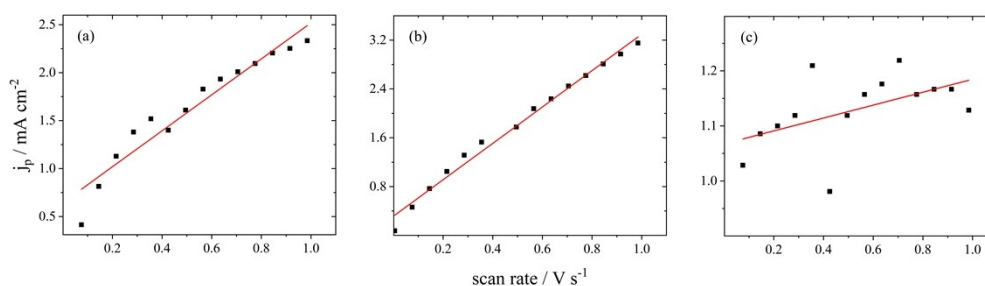


**Figure S10:**  $j_p$  vs. scan rate plot for peaks (a) I, (b) II and (c) III. Electrolyte: aqueous solution containing  $[\text{H}_2\text{SO}_4] = 0.5 \text{ mol L}^{-1}$  and  $[\text{H}_3\text{C-HCOH-CH}_3] = 1.0 \text{ mol L}^{-1}$ .

The adjustments presented in Figure S10 are just significantly better for peak II, and presented a slope of  $0.6 \text{ mF cm}^{-2}$ , for the other ones, not much was gained. For peak I the two linear

regions is still present, and for such plot, just the change in number of electrons would make sense. Finally, for the application of such model, Tafel-like plots ( $E_p$  vs.  $\log v$ ), are needed and, as can be seen in Figure S11, for all cases a slope of 25 mV was observed for peaks I and II.

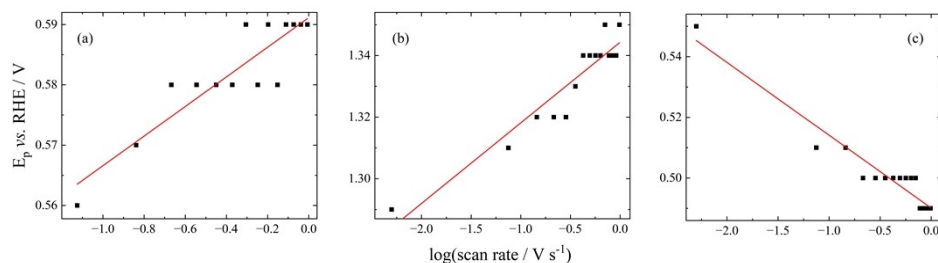


**Figure S11:**  $E_p$  vs. logarithm of scan rate plot for peaks (a) I, (b) II and (c) III. Electrolyte: aqueous solution containing  $[H_2SO_4] = 0.5 \text{ mol L}^{-1}$  and  $[H_3C-HCOH-CH_3] = 1.0 \text{ mol L}^{-1}$ .

In this way, it is expected that, even with different intermediates involved to each peak, since different behaviors were observed in Figure S10, the kinetics of both reactions are similar in  $n(1-\alpha)$ . For the third peak, the Tafel-like-slope was  $-25 \text{ mV}$ , once again, suggesting similarities in the kinetics. The negative signal is probably related to the fact that it is observed during the negative scan.

## References

- 1 B. B. Damaskin and A. N. Frumkin, *Modern Aspects of Electrochemistry*, London, 1964, vol. 3.
- 2 Gileadi E., *Electrode Kinetics for Chemists, Chemical Engineers, and Materials Scientists*, New York, 1993.
- 3 S. Srinivasan and E. Gileadi, The Potential-Sweep Method: A Theoretical Analysis, *Electrochim Acta*, 1966, **11**, 321–335.